International Journal of Progressive Sciences and Technologies (IJPSAT)
ISSN: 2509-0119.

http://ijpsat.ijsht-journals.org
Vol. 20 No. 1 April 2020, pp. 109-122

Comparative Theoretical Study on the Electronic Structures of the Isolated Molecular Gyroscopes with Polar and Nonpolar Phenylene Rotator

Anant Babu Marahatta[1, 2,*] and Hirohiko Kono[3]

[1]Department of Chemistry, Amrit Science Campus, Tribhuvan University, Kathmandu, Nepal

[2]Chemistry Subject Committee, Kathford International College of Engineering and Management (Affiliated to Tribhuvan University), Kathmandu, Nepal

[3]Department of Chemistry, Graduate School of Science, Tohoku University, Sendai, Japan

Abstract – Over the past decade, an assembly of the molecular components that produces quasi-mechanical movements in response to specific stimuli has become an intriguing research area. Interestingly, a rationally designed and strategically synthesized macroscopic gyroscope like molecular model with a closed topology has already demonstrated such remarkable behavior of the molecular machine. As its representative examples, the chemically synthesized siloxaalkane molecular gyroscopes (SMGs) with polar (e.g. ROT-2F and ROT-2Cl) and nonpolar (e.g. ROT-2H) rotating units (rotators) are considered here, and investigated their ground state electronic structures theoretically under non-crystalline condition by using density functional theory (DFT) model. We found this theoretical model has semiquantitatively reproduced one or more X-ray observed equilibrium structures of all the three SMGs. While comparing their DFT derived structures, the siloxaalkane spokes of the ROT-2F and ROT-2Cl are found to be deformed significantly as in experimental results, and this structural deformation is reconfirmed here by the DFT computed values of the "free volume" units present around each central rotator. The present DFT findings can be used to check whether its calculations are qualitatively agreed to the DFTB (Density Functional based Tight Binding) so that one can access the latter method directly while predicting reliable crystal structures and rotational dynamics of these SMGs under crystalline condition. This insight not only emphasizes the importance of molecular topology but also stresses the necessity of creating "free volume" unit around the central rotator to exhibit gyroscopic functions smoothly.

Keywords: Siloxaalkane Molecular Gyroscopes, Polar and Non-polar Rotators, Molecular Topology, Restricted and Unrestricted Rotation.

I. INTRODUCTION

The crystalline macrocyclic compounds with bridged π-electron systems have captivated much attention recently owing to their unique structures, dynamics and functions. These compounds are expected to possess many interesting physicochemical properties that can be functionalized in one's own interest. For example, a dipolar unit attached to the central phenylene ring encased within the static framework can be reoriented by conserving its volume under the influence of external stimuli [1], [2], [3]. Many recent experimental and theoretical investigations of such crystalline molecular systems have confirmed the internal rotation of the central phenylene (both substituted and non-substituted) units (i.e. rotator) with respect to a stationary macrocage (i.e. stator) (amphidynamic

Corresponding Author: Anant Babu Marahatta

behavior of the crystals) at temperatures ranging from high to moderate [3], [4], [5], [6], [7], [8], [9], [10], [11], [12]. This is why, these amphidynamic type molecular crystals are regarded as the promising nanomaterials carrying tremendous potentialities for developing varieties of smart, intelligent, and responsive materials. Among several experimentally synthesized amphidynamic types macrocyclic compounds, the crystalline molecular systems with a closed topology and having a large free space around the dipolar rotators are considered to be more practically significant due to their flexibility, functionality, and reliability while developing predesigned materials whose one or more properties can be significantly changed in a controlled fashion by external stimuli, such as electric field, magnetic field, light etc. During the past few years, Setaka *et al.* have been experimentally synthesizing the same type of molecular crystals having a typical molecular model shown in **chart 1a**, that seems quite analogous to macroscopic gyroscope (**chart 1b**) used in internal navigation system. Because of the structural similarity with the latter and to mimic some of its properties and functions, each molecule present in the crystalline network is referred as molecular gyroscope [4], [5], [6], [7], [8], [9], [10], [11], [12]. In this study, three different examples of the crystalline molecular gyroscopes with nonpolar rotator such as phenylene (hereafter, ROT-2H), and polar rotators such as difluorophenylene (hereafter, ROT-2F) and dichlorophenylene (hereafter, ROT-2Cl); each of which are alike to the molecular model given in the **chart 1a**; are considered individually and computed their ground state electronic structures under isolated molecular condition which is followed by their structural comparisons. Interestingly, the central unit of each of these molecular gyroscopes is encapsulated by the similar types of the siloxoalkane spokes (**chart 1c**), i.e. three molecular gyroscopes ROT-2H, ROT-2F, and ROT-2Cl are dissimilar to each other only by their central units themselves attached to the siloxaalkane framework through the spin axis as displayed in **chart 2**, where they are represented by **2a**, **2b**, and **2c** respectively.

Chart 1

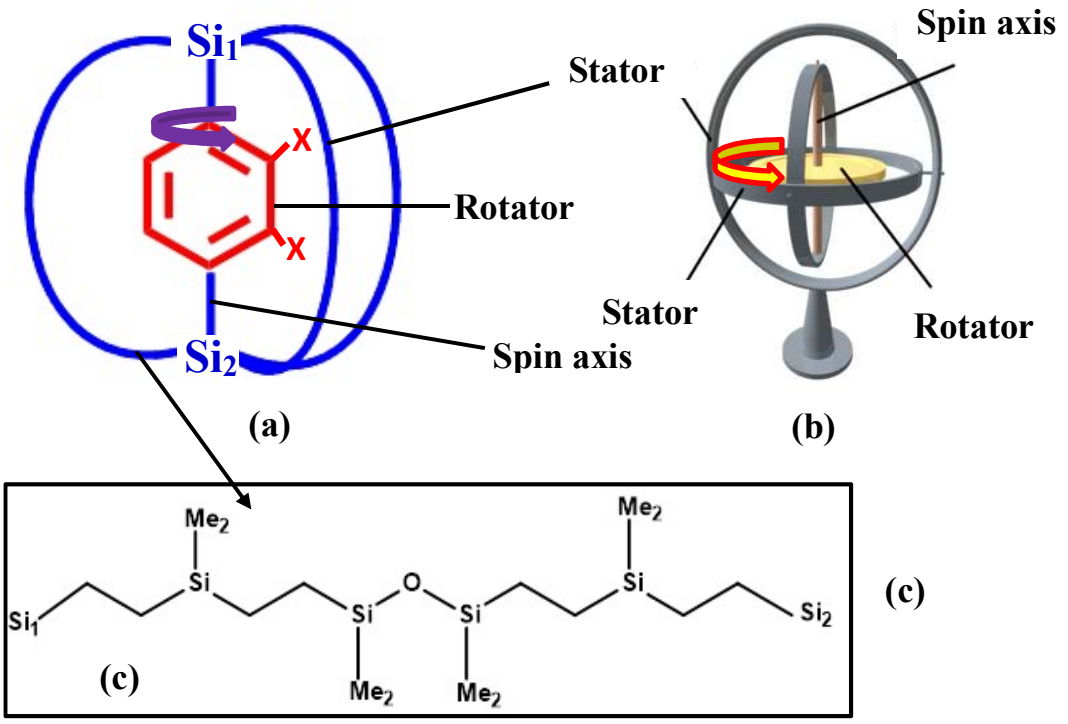

Setaka *et al.* firstly synthesized the non-polar molecular gyroscope **2a** [8], and then they introduced fluorine and chlorine atoms on its central phenylene unit for the purpose of designing dipolar molecular gyroscopes **2b**, and **2c** [9]. They have experimentally observed the smooth rotation of the phenylene and restricted rotation of the difluorophenylene units inside the static siloxaalkane spokes of the **2a**, and **2b** between three and two stable positions at T ≥ 223K and T= 273K respectively. In contrary, the rotary motion of the dichlorophenylene unit of the **2c** is not observed even though the type of the surrounding framework remains unchanged. Likewise, in comparison to the **2a**, a significant deformation in the shape of the siloxaalkane cages of its polar analogue **2b**, and **2c** are noticed. This structural deformation which is most probably caused due to substituting two hydrogen atoms of the central phenylene of **2a** by two fluorine (becomes **2b**) and two chlorine (becomes **2c**) may narrow down a "free volume" unit (the volume where the rotator is enclosed by the static framework inside which it moves more or less freely) present around the rotating segment. It may directly affect the rotational behavior of the central units such as restricted rotation as observed in **2b** or completely prevented rotation as in **2c**. The same consequences including the detailed structural changes occurring in the molecular gyroscopes before and after halogenating the central rotating unit of the **2a** and the role of the deformed siloxaalkane spokes to direct rotator at the confined position of the "free volume" unit can only be quantified if one could mostly reproduce the experimentally observed structures of the **2a**, **2b**, and **2c** by some computational means. It is absolutely true that the computationally/theoretically produced three dimensional view of the ground state electronic structures can ease the structural analytic process excessively which can further simplify "free volume" unit estimation technique quantitatively. These computational estimations not only provide a direct route for explaining the structural changes occurred in the **2b**, and **2c** in compare to **2a** but also ascertain their experimentally observed restricted or unrestricted or prevented type rotations. With these as major objectives, we are the first to apply a computationally robust density functional theory (hereafter, DFT) model to each **2a**, **2b**, and **2c** molecular gyroscope separately and generated their low energy electronic structures under the isolated molecular condition. Since, the DFT model is based on the electron density of a system through which the energetically most stable or ground state electronic structures/energies and properties of a system can be uniquely determined [13], [14] and has an enough ability to investigate ground state electronic structures of the multi-electron and/or many-body giant molecular systems [15], [16], [17], [18], [19], [20], [21]; it could be one of the most potent computational tools to reproduce experimentally observed molecular structure of each molecular gyroscope **2a**, **2b**, and **2c**. Despite many more notable limitations of this model with the main one being lack of complete mathematical treatment of dispersion or long-range Van der Waals type interaction [22], [23], [24], [25], [26], [27], its direct consequences is significant only while applying the DFT model to the systems that are dominated by dispersion (e.g. interacting noble gas atoms) [28] or where dispersion competes significantly with other effects (e.g. in biomolecular systems) [29]. In the molecular gyroscopes **2a**, **2b**, and **2c**, the same intramolecular nonbonding type interactions do exist (between central rotating unit and surrounding siloxaalkane arms), but it must play less decisive role (than in biomolecular systems) while converging the concerned trial structures into the most stable ground state electronic structures under non-crystalline condition. The structure of this paper is organized as: the theoretical approaches and computational methods are outlined in section 2, the results and discussions are presented in section 3, and the notable conclusions are given in section 4.

Chart 2 §

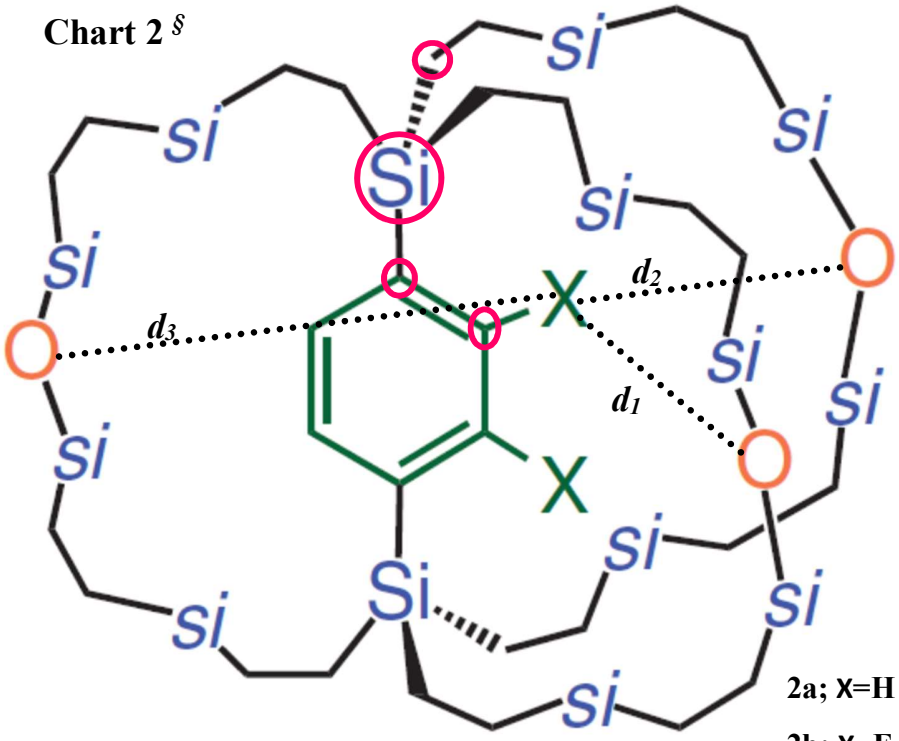

2a; X=H (ROT-2H)

2b; X=F (ROT-2F)

2c; X=Cl (ROT-2Cl)

§ It is reproduced from the supplementary material of reference 9. Two methyl groups attached to each Si atom (except Si_1 and Si_2) are omitted for clarity. The atoms encircled by pink color form the dihedral angle of the central phenylene rotator. The $d_{OX} = \{d_1, d_2, d_3\}$ estimates the "free volume" unit present around the rotator.

II. Computational Details

As the starting (trial) structures for geometry optimization of **2a**, **2b**, and **2c**, the initial coordinates of the atoms were taken directly from the X-ray crystallographic data provided by Professor Wataru Setaka from Tokushima Bunri University, Japan. For molecular gyroscope **2a**, the isolated molecule was extracted from the Cartesian coordinates of the unit cell geometry at 223 K (monoclinic crystal) and for **2b** and **2c**, the same was extracted from the unit cell geometry at 273 K (orthorhombic crystal). Since the molecular gyroscope **2a** is a precursor module of **2b**, and **2c**, it is taken here as a reference molecule. So, only its most stable equilibrium structure out of the three experimentally observed stable forms was optimized under the non-crystalline condition by using the DFT method, whereas for the molecular gyroscope **2b**, both of its degenerate equilibrium structures that are dissimilar to each other by 1π phenylene flipping positions were optimized. For simplicity, these two degenerate structures with different phenylene angular orientations inside the siloxaalkane cage are represented hereafter by structure **A** (dihedral angle = 0.56π) and structure **B** (dihedral angle = 1.57π) respectively. Unlike **2a** and **2b**, the molecular gyroscope **2c** whose dichlorophenylene

ring was not observed to be rotated experimentally has a single stable structure, and it was also optimized by the same computational means. To verify all these converged geometries as the energetically minimum structures, we also ran the frequencies calculation job (*Gaussian* keyword: *Freq*) computationally. For the DFT optimization process, all the *Gaussian* keywords and methodologies were selected as instructed in *Gaussian* 09 manual [30]. The hybrid functional based DFT method known as B3LYP was used with the basis set of this type: 6−31G (d, p) i.e. the methodology used was DFT: *B3LYP / 6−31G (d, p)*. The better and more reliable computational results were assured by using the greater basis set of the type 6−31G (d, p) where the "6−31G" is the standard, split-valence double-zeta basis set: the functions that were used in *Gaussian* script computationally while describing the core and valence orbitals of the atoms; and the functions in parentheses "(d, p)" are polarization functions on heavy atoms and hydrogen that was used to properly describe chemical bonds [31]. Again, to make *Gaussian* for running desirable computation, the molecular charge and spin multiplicity was specified as two integers accordingly. Here, all three molecular gyroscopes **2a**, **2b**, and **2c** are neutral molecules (charge = 0), and they are a spin-Singlet, with S = 0 and the multiplicity (2S + 1) = 1. Thus, the set of integers used to describe the neutral molecule was (0, 1). Moreover, while solving the electronic Schrodinger equation iteratively, the self-consistent field (hereafter, SCF) with both default SCF procedure (SCF=Tight) and Berny algorithm for optimizations to a local minimum were selected in *Gaussian* 09 [30] [32]. The *Gaussian* output files of each molecular gyroscope were read by using GaussView: the *Gaussian* graphical interface [33], and various chemical data displayed in three dimensions were extracted. All the DFT optimized geometries were displayed by using *Jmol*: an open source java viewer for chemical structures in three dimensions [34].

III. Results and Discussions

In general, theoretical calculations based on the DFT method provide trustworthy benchmarks for all other semi-empirical methods. In this study, we optimized the X-ray geometry of each molecular gyroscope **2a**, **2b**, and **2c** under non-crystalline condition (isolated molecule) using the *B3LYP/6−31G (d, p)* method and interpreted their equilibrium structures in reference to their X-ray produced geometries. At first, the most stable X-ray equilibrium structure (Figure 1(a)) of the molecular gyroscope **2a** was optimized without imposing any sorts of unit cell dimensions, and then both degenerate structures **A** and **B** of **2b** (Figure 2(a) and Figure 3(a)), and a single stable form of the **2c** (Figure 4(a)). The theoretically converged ground state electronic structures (no imaginary frequencies) of them are displayed in Figure 1(b), Figure 2(b), Figure 3(b), and Figure 4(b) respectively. Since the proper specification of the molecular geometries can only be drawn up if the structural parameters such as bond lengths, bond angles, and dihedral angles are known, some sets of them that are involved to determine the molecular geometries more precisely in the three dimensional space are carefully chosen here. The theoretically computed values of them for the central rotating units and the siloxaalkane arms of each molecular gyroscope **2a**, **2b**, and **2c** are listed along with the concerned experimental (X-ray determined) values in Table 1 and Table 2 respectively.

Table 1. X-ray vs. DFT optimized parameters for the central rotating units of the molecular gyroscopes 2a, 2b, and 2c.

Molecular Gyroscopes	Bonds	Bond length (nm)		"Free volume" unit (d_{OX}) (nm)		Rotator dihedral angle (π)[a]	
		X-ray	DFT	X-ray	DFT	X-ray	DFT
1. ROT-2F (**2b**) Structure **A**	C−F	0.144	0.141				
	C−C	0.138	0.139				
	C−H	0.093	0.110	$d_1 = 0.51$	$d_1 = 0.48$	0.56	0.63
	C−Si_1	0.189	0.187	$d_2 = 0.84$	$d_2 = 0.85$		
	C−Si_2	0.189	0.187	$d_3 = 0.95$	$d_3 = 0.92$		

Structure **B**	C−F	0.150	0.141			1.57	1.64
	C−C	0.138	0.139				
	C−H	0.093	0.110	$d_1 = 0.52$	$d_1 = 0.51$		
	$C-Si_1$	0.189	0.187	$d_2 = 0.84$	$d_2 = 0.86$		
	$C-Si_2$	0.189	0.187	$d_3 = 0.94$	$d_3 = 0.92$		
2. ROT-2Cl (**2c**)	C−Cl	0.174	0.141			0.32	0.30
	C−C	0.139	0.139				
	C−H	0.093	0.110	$d_1 = 0.81$	$d_1 = 0.83$		
	$C-Si_1$	0.189	0.187	$d_2 = 0.84$	$d_2 = 0.83$		
	$C-Si_2$	0.191	0.187	$d_3 = 0.87$	$d_3 = 0.79$		
3. ROT-2H (**2a**) (reference molecule)	C−C	0.140	0.141			0.55	0.31
	C−H	0.094	0.111	$d_1 = 0.39$	$d_1 = 0.41$		
	$C-Si_1$	0.188	0.188	$d_2 = 0.43$	$d_2 = 0.41$		
	$C-Si_2$	0.188	0.188	$d_3 = 0.51$	$d_3 = 0.52$		

The detailed analyses of the different kinds of bonds and their lengths associated with the central rotating units of **2a**, **2b**, and **2c** listed in the second and third column of Table 1 suggest that the respective central phenylene, difluorophenylene, and dichlorophenylene rings have some degree of electrons delocalization. This is because all the C−C bond lengths of both types of phenylene units (halogen substituted and non-substituted) are intermediate while comparing them with the length of a C=C double bond (bond length = 0.135 nm) and a C−C single bond (bond length = 0.147 nm) in ethene and ethane respectively; which further indicates that each central unit has partial double bond characters where the electrons are not associated with any single atom or single covalent bond but are likely to be found equally anywhere along all the chemical bonds. Moreover, due to the presence of the three siloxaalkane arms around the central rotating unit of each molecular gyroscope, some nonbonding type interactions (though of weak strength) take place between them that may also distort the shape of each central unit from its regular planar structure as can be seen in each X-ray as well as DFT derived geometries. This interaction is most commonly called steric effects that arises from the repulsive forces between the overlapping electron clouds of each central unit and the surrounding siloxaalkane spokes. Such steric hindrance not only creates constraints but also internally forces the central phenylene unit of each molecular gyroscope **2a**, **2b**, and **2c** for adjusting into the particular conformation of the free space present within the static siloxaalkane spokes. That is why, the interior and exterior bond angles and the torsional angles of each central phenylene unit are distorted from the concerned values of the planar benzene molecule (these values are omitted in Table 1 as they are considered to be less significant in this study). As can be seen in the fifth column of Table 1, the phenylene dihedral angle for the experimentally produced most stable structure of **2a** is 0.55π (modulo π), the difluorophenylene dihedral angle for the two X-ray equilibrium structures of **2b** are 0.56π and 1.57π (1π flip), of which structures or dihedral angles are denoted by **A**, and **B**, respectively and the dichlorophenylene dihedral angle of the single equilibrium structure of **2c** is 0.32π. By the DFT method, these angles are converged to 0.31π, 0.63π↔1.64π (1π flip), and 0.30π respectively. It reflects that the experimentally observed degenerate structures **A** and **B** of **2b** that are related to each other by 1π flipping of the difluorophenylene unit are theoretically confirmed. Additionally, as can be seen in Table 1, all the DFT derived bond length data sets for the central phenylene units of each molecular gyroscope are quite consistent with the X-ray produced data sets.

[a] It is formed by the atoms that are encircled by pink color in chart 2.

It is obvious that an available space ("free volume" unit) present inside the static siloxaalkane spokes gives freedom to the rotating unit. But, due to the flexible nature of such spokes that causes them to squeeze inward, there is a high chance of narrowing down the pre-existing inner space around the rotator, and hence increases the intensity of the intra-molecular type interactions between the rotator and spokes, which ultimately makes the hindered type rotation. In other words, the rotator can only rotate smoothly if it experiences minimum rotational

energy barrier. It means that there is a direct relation between the "free volume" unit, rotational energy barrier, and types of rotation (restricted, unrestricted, and prevented as in ROT-2F, ROT-2H, and ROT-2Cl respectively). That is why, it is very essential to approximate the "free volume" unit present around the rotator of the theoretically converged equilibrium structure of each molecular gyroscope **2a**, **2b**, and **2c**. If we carefully examine the molecular model given in chart 2, the "free volume" unit is simply an intervening space that exists in between the O atom of each siloxaalkane arm and the nearest X (H in **2a** or F in **2b** or Cl in **2c**) atom of the central phenylene ring each of which is assigned by d_1, d_2, and d_3 in chart 2. Here, we have approximately estimated this unit by determining the O−X (X= H or F or Cl) distance $d_{OX} = \{d_1, d_2, d_3\}$ of each DFT derived structure, and compared each value to that of the corresponding X-ray structure. All the concerned theoretical d_{OX} values are listed in the fourth column of Table 1, where they are found to be in close agreement with the respective experimental values given in the same column. Thus, it guaranties theoretically that there is a presence of sufficient "free volume" unit around the rotator of each molecular gyroscope **2a**, **2b**, and **2c**.

More interestingly, if we compare the "free volume" units *i.e.* $d_{OX} = \{d_1, d_2, d_3\}$ values of the **2b** and **2c** to each other as well as to the reference molecule **2a**, it is very easy to explain the X-ray observed structural deformation of the siloxaalkane spokes in the first two molecular gyroscopes in reference to the last one. As a rule, the closest distance that the two atoms can approach one another is given by the sum of their van der Waals radii. In other words, the minimum distance d_{OX} between O and X atoms should be greater than the sum of their van der Waals radii so that a sufficient clearance around the rotator is maintained. As the van der Waals radii of H, F, Cl, (X) and O atoms are 0.12 nm, 0.147 nm, 0.175 nm, and 0.152 nm respectively, the measured d_{OX} values of **2a**, **2b**, and **2c** highly exceeds the sum of the van der Waals radii of the concerned atoms. Along with this, the van der Waals radii of the H, F, and Cl atoms further speculate their atomic size that goes on increasing from H to Cl. It means, while substituting two H atoms of the phenylene rotator of **2a** by two F (as in **2b**) and two Cl (as in **2c**) atoms, the central rotator becomes more bulky and unequal in size. This is why, an equal amount of the "free volume" unit is insufficient to each molecular gyroscope **2a**, **2b**, and **2c**, i.e. the largest free space is required inside the siloxaalkane spokes of **2c** to accommodate more bulky dichlorophenylene, and then to difluorophenylene of **2b** than the pheylene rotator of **2a**. Thus, the most bulky dichlorophenylene, and the second most bulky difluorophenylene central units obviously push the surrounding siloxaalkane framework quite away from the center, resulting the outward inflation of the siloxaalkane spokes or deformation of the whole gyroscopic structures from its original framework of the precursor module (reference molecule) **2a**. It can further be clarified by saying that the halogenated phenylene units present in **2b** and **2c** create comparatively strong steric effects to the surrounding siloxaalkane chains which when avoiding such steric hindrance dilates outward giving the deformed molecular structure as theorized by the increasing trends of the $d_{OX} = \{d_1, d_2, d_3\}$ data sets (d_{OX}: **2a < 2b < 2c)** given in the fourth column of Table 1. The same is the reason why the phenylene unit of the **2a** undergoes smooth and facile rotation (low rotational barrier) in three stable positions, the difluorophenylene unit of the **2b** has restricted rotation (comparatively high rotational barrier) in two stable positions only, and the dichlorophenylene unit of the **2c** remains at a single position (prevented rotation) whenever the temperature is less than 273K. The rotation of the dichlorophenylene unit of the **2c** becomes unfavorable structurally as well due to its size, and inappropriate and unfriendly orientation of the two Cl atoms towards the three siloxaalkane arms as can be seen in Figure 4. The detailed about the rotational barriers, and the rotary dynamics of such crystalline molecular gyroscopes can only be computed theoretically by considering their unit cell geometries under a periodic boundary condition (hereafter, PBC). We have already reported about the same features for the molecular gyroscope **2a** elsewhere [35]. In future, they will be computed for the molecular gyroscopes **2b** and **2c**.

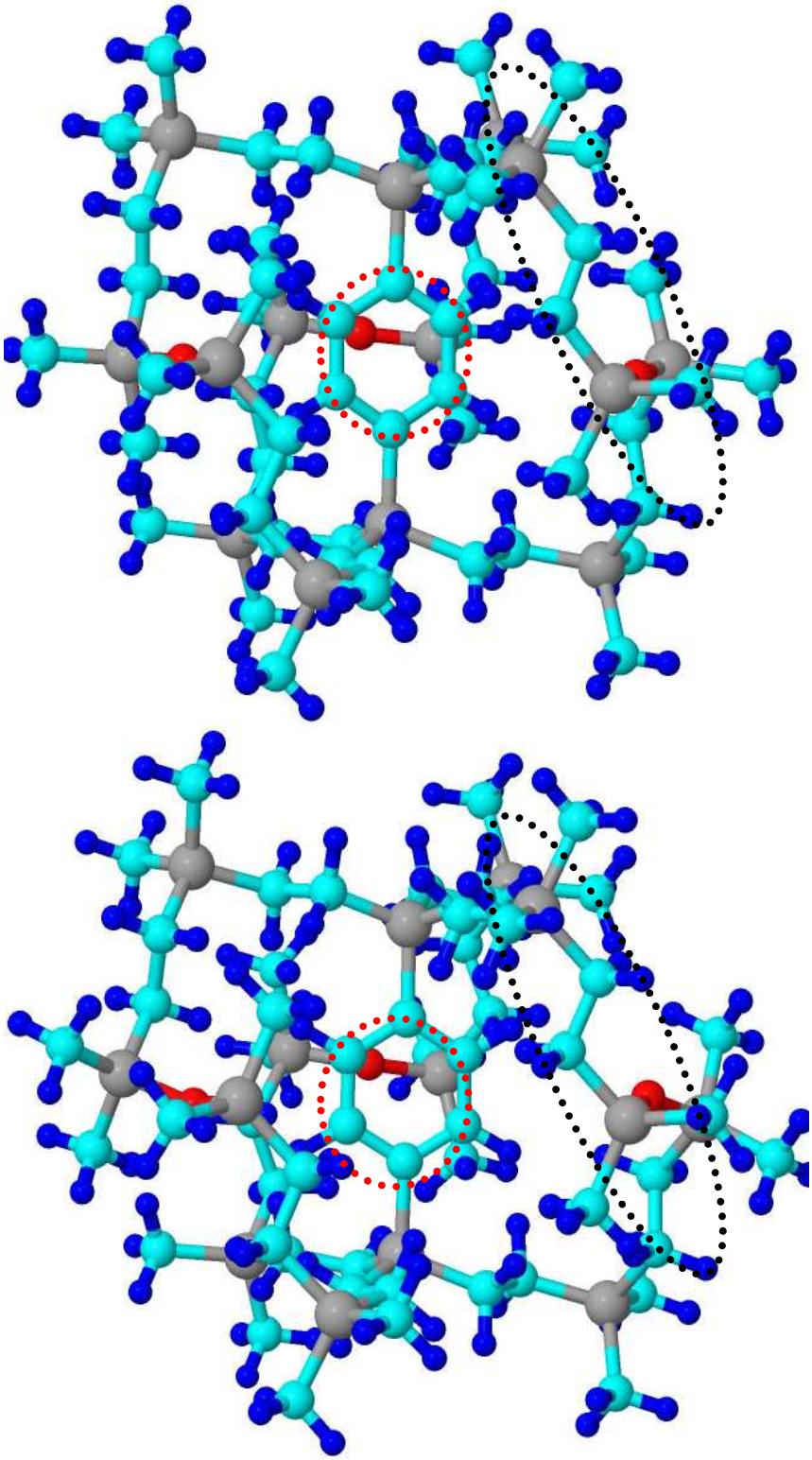

Figure 1. (a) X-ray (b) DFT optimized geometry of an isolated ROT-2H molecular gyroscope 2a. The cyan, blue, dark gray, and red spheroids represent Carbon, Hydrogen, Silicon, and Oxygen atoms respectively. The phenylene rotators and siloxaalkane arms are enclosed by red and black circles respectively.

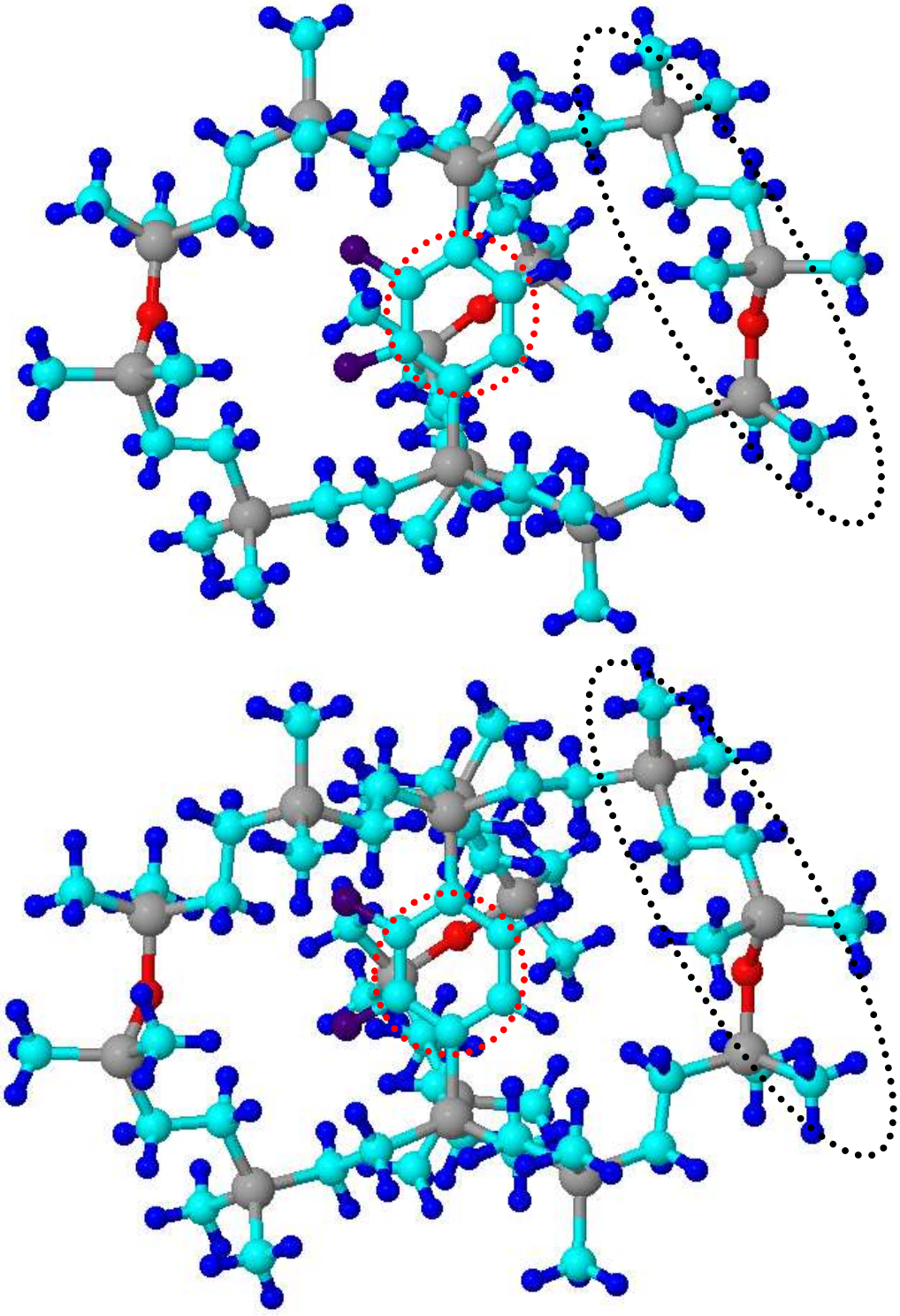

Figure 2. (a) X-ray (b) DFT optimized geometry of an isolated ROT-2F molecular gyroscope with difluorophenylene position A. The cyan, blue, dark gray, red, and indigo spheroids represent Carbon, Hydrogen, Silicon, Oxygen, and Flourine atoms respectively. The difluorophenylene rotators and siloxaalkane arms are enclosed by red and black circles respectively.

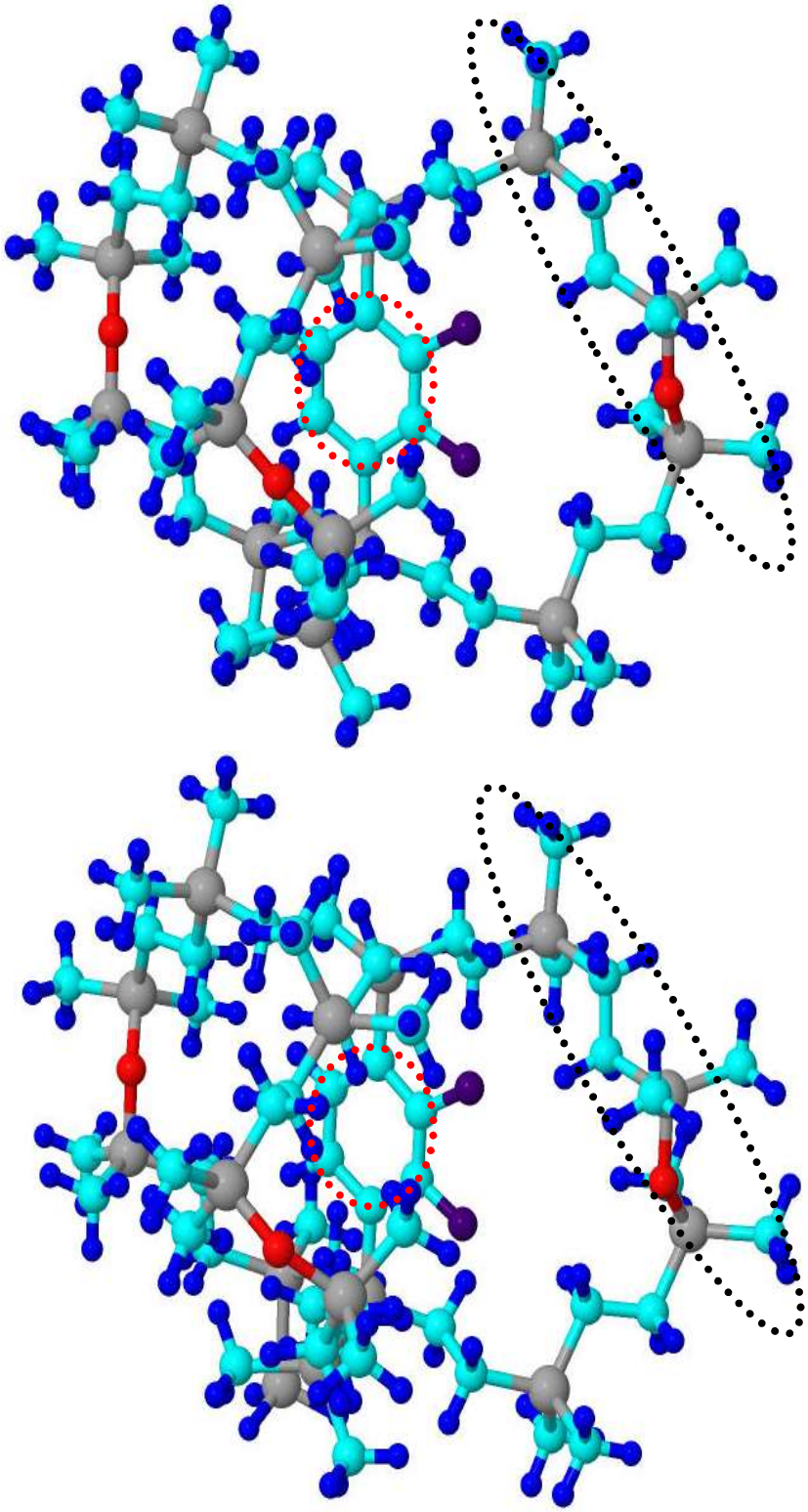

Figure 3. (a) X-ray (b) DFT optimized geometry of an isolated ROT-2F molecular gyroscope with difluorophenylene position B. The cyan, blue, dark gray, red, and indigo spheroids represent Carbon, Hydrogen, Silicon, Oxygen, and Flourine atoms respectively. The difluorophenylene rotators and siloxaalkane arms are enclosed by red and black circles respectively.

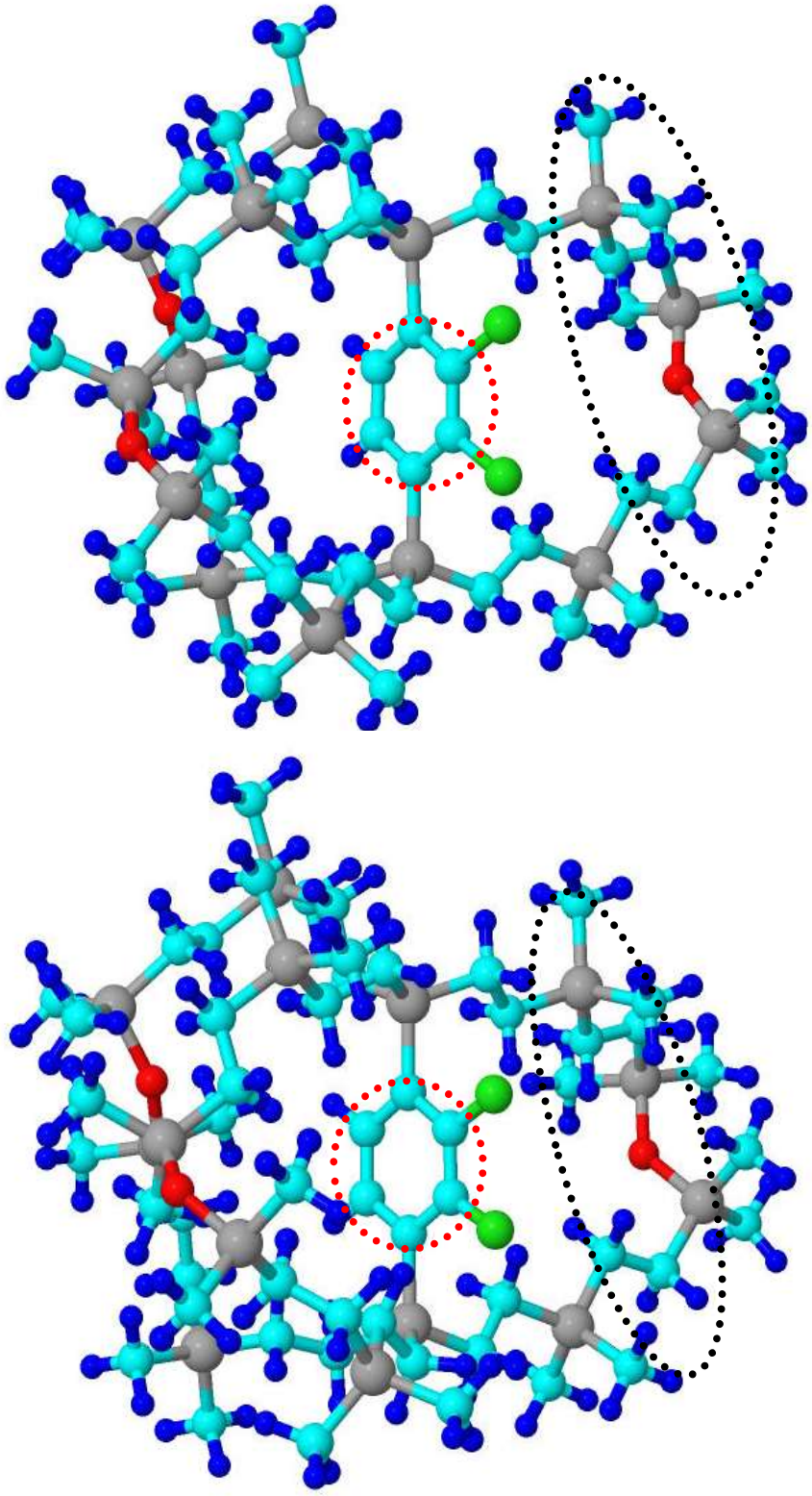

Figure 4. (a) X-ray (b) DFT optimized geometry of an isolated ROT-2Cl molecular gyroscope. The cyan, blue, dark gray, red, and green spheroids represent Carbon, Hydrogen, Silicon, Oxygen, and Chlorine atoms respectively. The dichlorophenylene rotators and siloxaalkane arms are enclosed by red and black circles respectively.

Similarly, the detailed analyses of the different kinds of bond lengths present in the siloxaalkane chains of **2a**, **2b**, and **2c** listed in the third column of Table 2 confirm that there is no any significant changes in the specific bond lengths associated with C atom occur while replacing phenylene rotator of **2a** by the difluorophenylene or dichlorophenylene. In contrary, the three sets of Si−O−Si bond angles and Si−O bond lengths in three siloxaalkane arms do vary slightly. This is because of their flexible property which is, however considered as very significant experimentally while accommodating more bulky rotating units (difluorophenylene or dichlorophenylene) inside the available "free volume" unit. As explained in previous paragraph, the structural outward dilation caused by the size of the halogen atoms attached to the central phenylene unit may also enforce the surrounding siloxaalkane chains for varying bond lengths and angular parts of their most flexible regions such as Si−O−Si and Si−O. Again, if we compare all of these structural data sets of the siloxaalkane arms derived from the X-ray and the DFT method individually, the main discrepancies are also present in the experimental and theoretical Si−O−Si bond angles and Si−O bond lengths. However, this is in good agreement if we consider the flexibility of the Si−O−Si linkages and Si−O segments. The partial ionic and double bond characters of such linkages not only govern their strength but also contribute to exceptional conformational flexibility of the $-(Si-O)_x-$ chains and their segments [36]. In turn, these characteristics are not only responsible for creating elasticity of the whole siloxaalkane spokes but also for easing the synthetic procedure of different types of functional molecular gyroscopes with variable sized rotating segments. Setaka *et al.* have clearly mentioned elsewhere [8], [9], [10] that they were benefited by the same behavior of the surrounding siloxaalkane spokes while designing and synthesizing **2b** and **2c** molecular gyroscopes from their original precursor module **2a**.

Table 2. X-ray vs. DFT optimized parameters for each siloxaalkane arm of the molecular gyroscopes 2a, 2b, and 2c

Molecular gyroscopes	Si-O-Si angle (π)		Bonds	Bond lengths (nm)	
	X-ray	DFT		X-ray	DFT
1. ROT-2F (**2b**) Structure **A**	0.97	0.78	C−C	0.153	0.153
	0.84	0.75	C−H	0.097	0.110
	0.84	0.74	C−Si	0.188	0.187
			Si−O	0.163	0.175
Structure **B**	0.97	0.78	C−C	0.153	0.153
	0.84	0.75	C−H	0.097	0.110
	0.84	0.74	C−Si	0.187	0.188
			Si−O	0.159	0.175
2. ROT-2Cl **(2c)**	0.79	0.74	C−C	0.155	0.153
	0.80	0.76	C−H	0.097	0.110
	0.83	0.79	C−Si	0.188	0.186
			Si−O	0.164	0.175
3. ROT-2H **(2a)** (reference molecule)	0.91	0.78	C−C	0.150	0.152
	0.94	0.78	C−H	0.097	0.109
	0.96	0.82	C−Si	0.180	0.180
			Si−O	0.160	0.172

As a whole, if we compare the experimental and DFT optimized structures of each isolated siloxaalkane molecular gyroscope **2a**, **2b**, and **2c** shown in Figure 1 to Figure 4, we reconfirm the above mentioned features for the optimized structures that the orientation of the central phenylene units and the conformations of the surrounding siloxaalkane spokes are well reproduced. Besides that the orientation and conformation of the methyl groups attached to each siloxaalkane arm are also not noticeably different. The small inconsistencies appeared in the DFT optimized structures are due to lacking proper

mathematical formulation in the DFT model for evaluating the effect of small dispersion type force that exists in between the central phenylene unit and the surrounding siloxaalkane spokes (enclosed by red and black circles respectively in Figure 1 to Figure 4). A more realistic ground state electronic structure for each of these crystalline molecular gyroscopes can only be produced by realizing their unit cell geometries computationally under the PBC. However, the DFT model is considered to be comparatively irrelevant to determine the structure of the crystalline compounds. But, another theoretical approach (i.e. Density Functional based Tight Binding (DFTB) method) that was already developed on the basis of DFT's fundamental principle is found to be highly relevant. See our previous publications [35], [37], [38] for the performance of the DFTB approach to derive crystal structure of the molecular gyroscope **2a**. In future, we will apply same method to **2b**, and **2c** for their detailed structural investigations under the PBC. For this, the present DFT findings must be used to check whether its calculations are qualitatively agreed to the DFTB or not.

IV. Conclusion

We applied first principles DFT method to the experimentally synthesized siloxaalkane molecular gyroscopes with polar (difluorophenylene and dichlorophenylene: ROT-2F and ROT-2Cl) and non-polar (phenylene: ROT-2H) rotating segments under non-crystalline condition, and computed their ground state electronic structures theoretically. As the molecular gyroscope ROT-2H is a precursor module of the ROT-2F and ROT-2Cl, the former one has been taken here as a reference molecule to unveil the structural inconsistencies between themselves. Therefore, only the most stable X-ray structure of the ROT-2H is optimized among its three experimentally observed stable forms, whereas for the ROT-2F and ROT-2Cl, two degenerate equilibrium structures of the former and a single stable form of the latter are optimized separately. We successfully located all of these X-ray observed equilibrium structures theoretically and found themselves quite resembled to the concerned experimental structure. In accordance with it, most of the structural data sets for each molecular gyroscope are also in good agreement with the concerned X-ray data sets. However, the small inconsistencies appeared on the $-(Si-O)_x-$ chains and their segments of each siloxaalkane arm of each molecular gyroscope are due to the presence of partial ionic and double bond characters of the Si−O−Si linkages that in turn contributes them to acquire the exceptional conformational flexibility. Likewise, a comparatively more deformed shape of the siloxaalkane cage of the ROT-2F and ROT-2Cl (in compare to ROT-2H) is theoretically confirmed by estimating the “free volume” units present in between the central rotating segments and the surrounding siloxaalkane spokes. We observed this structural deformation most likely arises while avoiding steric hindrance of the central halogen substituted phenylene ring by the surrounding siloxaalkane spokes. The same steric effect is responsible for establishing a sufficient space around the halogen substituted phenylene units of the ROT-2F and ROT-2Cl so that more bulky rotating units of them can be accommodated easily within the siloxaalkane spokes of their precursor module ROT-2H.

As our present research is mainly aimed to execute comparative theoretical studies on the ground state electronic structures of the molecular gyroscopes ROT-2H, ROT-2F, and ROT-2Cl under non-crystalline condition by employing computationally efficient DFT method, we have not considered their unit cell geometries under periodic boundary condition (PBC) this time as it is computationally undoable with the DFT method. We believe this insight has provided reasonably a simple approach for characterizing isolated gyroscopic molecular structures and interpreting the effect of bulky rotating segments to deform the original gyroscopic structure of the precursor molecule. All the DFT findings presented here have demonstrated that more advanced quantum mechanical method itself derived from the DFT such as Density Functional based Tight Binding (DFTB) method would be very suitable to predict reliable crystal structures and microscopic rotary motion of such crystalline molecular gyroscopes, as this method is especially formulated for modeling molecular crystals and simulating their dynamics by extensively reviewing DFT method. See our previous publications (reference [35], [37], and [38]) for the performance of the DFTB method to derive crystal structures and rotary dynamics of the molecular gyroscope ROT-2H.

Acknowledgement

Professor Wataru Setaka from Tokushima Bunri University, Japan is highly acknowledged for providing X-ray data sets of each crystalline siloxaalkane molecular gyroscope: ROT-2H, ROT-2F, and ROT-2Cl. Being an active collaborator and contributor to our first research project that was aimed to investigate the crystal structure and rotational dynamics of the

ROT-2H, the then his constructive discussions with us became commendable this time as well.

REFERENCES

[1] V. Balzani, M. Venturi and A. Credi, Molecular Devices and machines: A Journey into the Nano World (Wiley-VCH: Weinheim, 2003).
[2] T. R. Kelley, Molecular Machines. Topics in Current Chemistry (Springer, 2005).
[3] Z. Dominguez, H. Dang, M. J. Strouse and M. A. Garcia-Garibay, *J. Am. Chem. Soc.* 124, 7719 (2002).
[4] M. A. Garcia-Garibay and C. E. Godinez, *Cryst. Growth Des.* 9, 3124 (2009).
[5] R. D. Horansky, L. I. Clarke, J. C. Price, T. V. Khuong, P. D. Jarowski and M. A. Garcia-Garibay, *Phys. Rev. B* 72, 014302 (2005).
[6] R. D. Horansky, L. I. Clarke, J. C. Price, S. D. Karlen, P. D. Jarowski, R. Santillan and M. A. Garcia-Garibay, *Phys. Rev. B* 74, 054306 (2006).
[7] Z. J. O'Brien, A. Natarajan, S. Khan and M. A. Garcia-Garibay, *Cryst. Growth Des.* 11, 2654 (2011).
[8] W. Setaka, S. Ohmizu, C. Kabuto and M. Kira, *Chem. Lett.* 36, 1076 (2007).
[9] W. Setaka, S. Ohmizu and M. Kira, *Chem. Lett.* 39, 468 (2010).
[10] W. Setaka and K. Yamaguchi, *Proc. Natl. Acad. Sci.* 109, 9271 (2012).
[11] A. V. Akimov and A. J. Kolomeisky, *J. Phys. Chem. C* 115, 13584 (2011).
[12] J. Michl and E. C. H. Sykes, *Am. Chem. Soc. Nano.* 3, 1042 (2009).
[13] M. C. Payne, M. P. Teter, D. C. Allan, T. A. Arias and J. D. Joannopoulos, *Rev. Mod. Phys.* 64, 1045 (1992).
[14] B. B. Yehuda and Y. Avishai, Quantum Mechanics with Applications to Nanotechnology and Information Science (ScienceDirect, 2013).
[15] J. B. Adams, Encyclopedia of Materials: Science and Technology (Elsevier, 2001).
[16] A. B. Marahatta, *Int. J. Prog. Sc. Tech.* 16 (1), 51 (2019).
[17] A. B. Marahatta, *Int. J. Prog. Sc. Tech.* 16 (2), 01 (2019).
[18] A. B. Marahatta, *Int. J. Prog. Sc. Tech.* 17 (1), 55 (2019).
[19] A. B. Marahatta, *Int. J. Prog. Sc. Tech.* 18 (2), 43 (2020).
[20] A. B. Marahatta, *Int. J. Prog. Sc. Tech.* 19 (1), 100 (2020).
[21] A. B. Marahatta, *Int. J. Prog. Sc. Tech.* 19 (2), 48 (2020).
[22] A. J. Cohen, P. M. Sánchez and W. Yang, *Science* 321, 792 (2008).
[23] A. D. Buckingham, P. W. Fowler and J. M. Hudson, *Chem. Rev.* 88 (6), 963 (1988).
[24] J. Tao, J. P. Perdew and A. Ruzsinszky, *Proc. Natl. Acad. Sci.* U. S. A. 109 (1), 18 (2012).
[25] A. D. Becke, *J. Chem. Phys.* 98, 5648 (1993).
[26] J. P. Perdew, K. Burke and M. Ernzerhof, *Phys. Rev. Lett.* 77, 3865 (1996).
[27] J. Tao, J. P. Perdew, V. N. Staroverov and G. E. Scuseria, *Phys. Rev. Lett.* 91, 146401-1 (2003).
[28] V. Mourik, T. Gdanitz and J. Robert, *J. Chem. Phy.* 116 (22), 9620 (2002).
[29] J. Vondrášek, L. Bendová, and V. Klusák, *J. Am. Chem. Soc.* 127 (8), 2615 (2005).
[30] Gaussian 09 manual. *http://gaussian.com/geom/?tabid=1#GeomkeywordReadOptimizeoption*
[31] J. B. Foresman and Æ Frisch, Exploring Chemistry with Electronic Structure Methods (Gaussian, Inc., 2015).
[32] Æ Frisch, Gaussian 09W Reference (Gaussian, Inc., 2009).
[33] Æ. Frisch, H. P. Hratchian, R. D. Dennington II, T. A. Keith and J. Millam, Gauss view 05 Reference (Gaussian, Inc. 2009).
[34] Jmol: an open-source Java viewer for chemical structures in 3D. *http://www.jmol.org/*
[35] A. B. Marahatta, M. Kanno, K. Hoki, W. Setaka, S. Irle and H. Kono, *J. Phys. Chem. C* 116, 24845 (2012).
[36] G. J. Richard and C. Julian, Silicon-Containing Polymers: The Science and Technology of Their Synthesis and Applications, pp.186-187, (Springer publication, 2000).
[37] A. B. Marahatta and H. Kono, *Int. J. Inn. Res. Adv. Stud.* 6,180 (2019).
[38] A. B. Marahatta and H. Kono, *Int. J. Prog. Sc. Tech.* 15(2), 263 (2019).